Electric Power Systems Research 163 (2018) 18–27

Contents lists available at ScienceDirect

Electric Power Systems Research

journal homepage: www.elsevier.com/locate/epsr

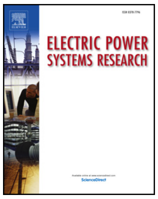

# Thermal and electrical performance assessments of lithium-ion battery modules for an electric vehicle under actual drive cycles

S. Panchal[a,*], M. Mathew[c], I. Dincer[a], M. Agelin-Chaab[a], R. Fraser[b], M. Fowler[c]

[a] *Department of Automotive, Mechanical & Manufacturing Engineering, Faculty of Engineering & Applied Science University of Ontario Institute of Technology, 2000 Simcoe Street North, Oshawa, Ontario, L1H 7K4, Canada*
[b] *Mechanical and Mechatronic Engineering Department, University of Waterloo, 200 University Avenue West, Waterloo, Ontario, N2L 3G1, Canada*
[c] *Chemical Engineering Departments, University of Waterloo, 200 University Avenue West, Waterloo, Ontario, N2L 3G1, Canada*

## ARTICLE INFO

*Keywords:*
Lithium-ion battery
Electric vehicle
Drive cycle
Temperature distribution
State of charge
Neural network

## ABSTRACT

In this paper, both thermal and electrical performance evaluations of a lithium-ion battery pack using real world drive cycles from an electric vehicle (EV) are presented. For the experimental measurements, a data logger is installed in the EV, and the real world drive cycles are collected. The EV has three lithium-ion battery packs consisting of a total of 20 battery modules in series. Each module contains six series × 49 parallel IFR 18650 cylindrical valence cells. The reported drive cycles consist of different modes: acceleration, constant speed, and deceleration in both highway and city driving at 2 °C, 10 °C and 17 °C ambient temperatures with all accessories on. Later, the same drive cycles are conducted in an experimental facility where four cylindrical lithium-ion cells are connected in series, and both electrical and thermal performances are evaluated. In addition, the battery model is developed using artificial neural network, which is validated with the real world drive cycles. The validation is carried out in terms of voltage, state of charge (SOC), and temperature profiles for all the collected drive cycles. The present model closely estimates the profiles observed in the experimental data. Moreover, with this study, the mathematical function for the average temperature, SOC, and voltage prediction are developed with weights and bias values.

## 1. Introduction

Automotive manufacturers are under extreme pressure to improve fuel economy and reduce emissions of their cars. In conjunction with this, they have to create and apply recent advancements to meet regulations. Electric vehicles (EVs), along with fuel cell vehicles (FCVs) and hybrid electric vehicles (HEVs), are seen as the answer to energy and environmental issues and they are more energy proficient [1,2]. In EVs, since the electric motors and inverters are utilized in the drive systems, in comparison with internal combustion engines, they have real points of interest. For example, fast torque reaction and control over every wheel [3]. The heart of EVs is the battery or battery pack. Among accessible technologies, the lithium-ion battery plays a key part in the improvement of EVs, HEVs, and PHEVs [4] as a result of their broad use because of: (1) high specific energy and power densities [5,6]; (2) high nominal voltage and low self-discharge rate [7]; and (3) long cycle-life and no memory effect [8]. However, lithium-ion batteries must be precisely observed and managed (electrically and thermally) to avoid safety (inflammability) and performance related issues [9,10].

This section gives a brief overview of lithium-ion battery structure, components and types. A lithium-ion battery cell usually has five distinctive layers, in particular: the negative current collector, negative electrode (anode), separator, positive electrode (cathode), and positive current collector. There are generally four sorts of positive electrode materials [11]: (a) a metal oxide with layered structure, for example, lithium cobalt oxide ($LiCoO_2$/LCO) [12]; (b) a metal with a three dimensional spinal structure, for example, lithium manganese oxide ($LiMn_2O_4$) [13]; (c) lithium nickel manganese cobalt oxide ($LiNiMnCoO_2$/NMC); and (d) a metal with a olivine structure, such as lithium iron phosphate ($LiFePO_4$/LFP) [14]. The anode is generally made of graphite or a metal oxide. The electrolyte can be liquid, polymer or solid. There are various types of lithium-ion batteries available such as cylindrical, and prismatic. The prismatic batteries are used for high capacity rating such as in automobiles [15].

In EVs and HEVs, the thermal management of lithium-ion batteries is a tremendous challenge because of the dynamic utilization of the battery cells and the extensive range of environments under which they work [16]. In a high temperature environment, lithium-ion batteries quickly degrade, while in a cold temperature environment, the power

---

[*] Corresponding author.
*E-mail addresses:* satyam.panchal@uwaterloo.ca, satyam.panchal@uoit.ca (S. Panchal).

https://doi.org/10.1016/j.epsr.2018.05.020
Received 7 February 2017; Received in revised form 23 February 2018; Accepted 22 May 2018

**Nomenclature**

| | |
|---|---|
| $e$ | $e$ is the number also called as Napier's Number and its approximate value is 2.718281828 |
| $H_k^1$ to $H_k^8$ | Hidden layer neuron from 1 to 8 |
| $I$ | Current [A] |
| $i$ | Index of hidden layer nodes |
| $j$ | Index of input layer nodes |
| $k$ | Index of time interval |
| $l$ | Index of output layer nodes |
| $N_H$ | Number of neurons in the hidden layer |
| $N_I$ | Number of neurons in the input layer |
| $N_o$ | Number of neurons in the output layer |
| $t$ | Time [s] |
| $W_{i,j}$ | Weights of connection between hidden layer neuron and output layer neurons |
| $x$ | Weighted sum of inputs from the preceding layers |
| $\beta_1$ to $\beta_8$ | Bias of hidden layer neurons from 1 to 8 |
| $\Gamma$ | Average temperature of all 20 module |
| $\theta_k$ | Time recorded from EV in second |
| $\mu$ | Bias associated with the output layer neuron |
| $\xi_k$ | Battery current recorded from EV in Amp |
| $\pi$ | Pi |
| $\sigma(.)$ | Activation function |
| $\omega_{i,j}$ | Weights of connection between input layer neuron and hidden layer neurons |
| $\infty$ | Infinity |

*Subscripts*

| | |
|---|---|
| act | Actual |
| *chg* | Charge |
| *dis* | Discharge |
| *int* | Internal |
| *sim* | Simulated |
| *oc* | Open circuit |
| *out* | Output |

*Superscripts*

| | |
|---|---|
| $T$ | Transpose of a matrix |
| $x$ | power value of the exponent e |

*Acronyms*

| | |
|---|---|
| ANN | Artificial neural network |
| BC | Boundary condition |
| BMS | Battery management system |
| BTMS | Battery thermal management system |
| C | Capacity |
| CC | Constant-current |
| CV | Constant-voltage |
| DAQ | Data acquisition |
| EV | Electric vehicle |
| FCV | Fuel cell vehicle |
| IFR 18650 | "I" stands for Li-ion rechargeable, "F" stands for the element "Fe" which is Iron, "R" just means the cell is round, 18650 means 18 mm diameter and 650 means 65 mm height |
| $LiCoO_2$ | Lithium cobalt oxide |
| $LiMn_2O_4$ | Lithium manganese oxide |
| $LiNiMnCoO_2$ | Lithium manganese cobalt oxide |
| $LiFePO_4$ | Lithium iron phosphate |
| LCO | Lithium cobalt oxide |
| LFP | Lithium phosphate |
| LPM | Lumped parameter model |
| LPV | Linear parameter varying |
| LM-ANN | Levenberge–Marquardt artificial neural network |
| MSE | Mean square error |
| NN | Neural network |
| NMC | Lithium manganese cobalt oxide |
| OCP | Open circuit potential |
| PSAT | Power train system analysis tool kit |
| PHEV | Plug-in hybrid electric vehicle |
| PDE | Partial differential equation |
| R | Regression |
| RS-232 | Recommend standard number 232 |
| SOC | State of charge |
| TDI | Load box for battery testing |
| UQM | Power phase motor developed by UQM |

output and energy are reduced, which eventually brings about reduction of performance and driving range [17]. A typical temperature range is between 20 °C and 40 °C [18] for lithium-ion batteries, and an extended range is between −10 °C and +50 °C for their fair operation [16]. There are two common types of cooling: (i) air cooling, and (ii) water cooling. The water cooling option appears to be more compelling, because of higher specific heat content contrasted with air cooling. It occupies less volume, yet brings more complexities and high cost and weight [19]. The temperature increase in a lithium-ion battery during charging/discharging follows three processes: (1) the rate at which heat is created inside the cell, (2) the rate at which heat conducts within the cell to the outer surface, and (3) the rate at which heat is expelled from the cell's external surface to the environment. Heat dissipation to the surrounding relies on the cell geometry and also the cooling system performance [20]. Temperature estimations and the prediction of the lithium-ion cell temperature are addressed by various papers including analytical and numerical modeling [21,22].

Numerous numerical models have been developed to predict the dynamic behaviors of batteries. An EV designer may use battery models for sizing the required battery and predict the battery discharge. Battery models are likewise utilized for on-line self-learning performance and SOC estimation in battery thermal management system (BTMS) [23,24]. There are numerous papers in the open literature available for battery thermal modeling, utilizing diverse methodologies. For example, artificial neural network [21,22,25,26], finite element model (FEM) [27] or lumped parameter model (LPM) [28], the linear parameter varying (LPV) model [29], or the partial differential equation (PDE) model [30], and the power train system analysis toolkit (PSAT) or Autonomie [31]. Some more studies on SOC estimation based on drive cycles are also accessible in the open literature [32,33]. Utilizing smart tools, for example, artificial neural networks (ANNs) has ended up being effective tools for exact estimating of vehicle pace profile of moving vehicle. A neuro-genetic predictive tool was produced for predicting the short-term traffic activity on road [34]. Genetic algorithm (GA) was also additionally utilized for the both optimization and developing of ANN architectures for short-term traffic flow prediction [35]. An ANN in view of an exponential smoothing strategy was produced to come up with a precise intelligent tool for forecasting the traffic flow, and later confirmed the realness of their system by repeating the same simulations using a Levenberge-Marquardt ANN (LM-ANN) [36]. In another study, a neural network for real-time vehicle speed predictions showed the legitimacy of the strategy utilized [37]. Here, we used the same methodology called ANN for drive cycle modeling. Artificial neural networks are generally sorted out in layers